Analytica Chimica Acta 1094 (2020) 130–135

Contents lists available at ScienceDirect

Analytica Chimica Acta

journal homepage: www.elsevier.com/locate/aca

Controlled assembly of AIEgens based on a super-quadruplex scaffold for detection of plasma membrane proteins

Longyi Zhu , Yang Li, Lei Zhang, Yunjie Wen, Huangxian Ju , Jianping Lei *

State Key Laboratory of Analytical Chemistry for Life Science, School of Chemistry and Chemical Engineering, Nanjing University, Nanjing, 210023, PR China

HIGHLIGHTS

- A tetramolecular hairpin-conjugated super-quadruplex is designed as molecular switch.
- Oligonucleotide-grafted AIEgens were synthesized without fluorescence emission.
- The activated G-quadruplex scaffold could assemble AIEgens to induce fluorescence enhancement.
- The integrated system established a simple and sensitive strategy for detection of plasma membrane protein.

GRAPHICAL ABSTRACT

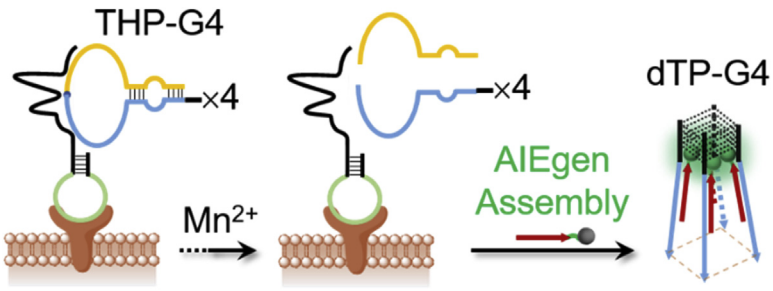

ARTICLE INFO

Article history:
Received 5 August 2019
Received in revised form
16 September 2019
Accepted 7 October 2019
Available online 11 October 2019

Keywords:
Biosensors
DNA quadruplexes
Aggregation-induced emission
Fluorescence
Plasma membrane protein
DNAzyme

ABSTRACT

Quantification of plasma membrane proteins (PMPs) is crucial for understanding the fundamentals of cellular signaling systems and their related diseases. In this work, a super-quadruplex scaffold was designed to regulate assembly of oligonucleotide-grafted AIEgens for detection of PMPs. The non-fluorescence oligonucleotide-grafted AIEgen (Oligo-AIEgen) was firstly synthesized by attaching the AIEgen to 3′-terminus of the oligonucleotide through click chemistry. Meanwhile, the tetramolecular hairpin-conjugated super-quadruplex (THP-G4) as cleavage element and signal enhancement scaffold composited of three elements: a substrate sequence of DNAzyme in the loop region, partial hybridization region in the stem, and six guanine nucleotides to form G-quadruplex. Once the DNAzyme was anchored on the specific PMPs through aptamer-protein recognition, the substrate sequence on the loop of THP-G4 was cleaved by DNAzyme with the aid of cofactor Mn^{II}, resulting in the conformation switch of THP-G4 to the activated G-quadruplex scaffold. The latter could assemble Oligo-AIEgens to generate aggregation-induced emission (AIE) enhancement, resulting in a simple and sensitive strategy for detection of membrane proteins. Moreover, the DNAzyme continuously cut the next THP-G4 to achieve recycling amplification. Under the optimized conditions, this AIE-based strategy exhibited good linear relationship with the logarithm of MUC1 concentration from 0.01 to 10 $\mu g\,mL^{-1}$ with the limit of detection down to 4.3 ng mL^{-1}. The G4-assembled AIEgens provides a universal platform for detecting various biomolecules and a proof-of concept for AIE biosensing.

1. Introduction

Plasma membrane protein (PMP) plays a vital role in many biological processes, such as materials transportation, intercellular

* Corresponding author.
E-mail address: jpl@nju.edu.cn (J. Lei).

https://doi.org/10.1016/j.aca.2019.10.010
0003-2670/

communication and intracellular signaling [1–4]. Perturbation in the expression levels of PMPs, as the result of abnormal cell metabolism, is associated with cancer and other fatal diseases [5–8]. Nowadays, various techniques are applied for PMPs detection with good performance [9–11], including surface-enhanced Raman scattering [12], fluorescence [13–15], colorimetric assays [16] and electrochemiluminescence immunoassays [17]. Particularly, fluorescence probes have been proved to be a promising approach due to their nondestructive interaction with target proteins and real-time quantification [18]. By enzymatic cleavage of substrate sequence conjugated on the green fluorescent protein, furin recognition and quantification were achieved on the membrane of living cells [19]. However, traditional fluorophore probes may suffer from aggregation caused quenching effect, and lead to the reduced signal for readout [20,21]. As a new kind of fluorescent emitter, aggregation-induced emission (AIE) was introduced in this work for quantification of PMPs due to the advantages of low background signal and good photostability.

Fluorogens with aggregation-induced emission characteristics (AIEgens) generate strong fluorescence emission in aggregate state due to the restriction of intramolecular motions [22]. AIEgen-based fluorescence probes are widely applied in biosensing and cell imaging with high brightness in aggregate state [23–27]. The fluorescence signal of AIEgens could be induced by electrostatic interaction [28], site-specific reactions [29], analyte binding [30] and environmental stimuli [31,32]. Specifically, the AIE probe consisting of sulfonic TPE derivatives with alkinyl group was turned on through click reaction for cell membrane imaging and photodynamic ablation [33]. An arginine-glycine-aspartic acid functionalized tetraphenylsilole was developed for sensitive detection of membrane protein integrin $\alpha_v\beta_3$ through ligand-receptor interaction [34]. The above multistep-synthesis of AIEgen-based bioprobes guarantees the selectivity and low limit of detection, and becomes a promising strategy for biomolecule detection.

DNA was extensively applied in designing versatile molecular switches because of its predictable structure, various biofunctions and flexible alteration of sequence [35–38]. In this work, a tetramolecular hairpin-conjugated super-quadruplex scaffold (THP-G4) was rationally designed to assemble oligonucleotide-grafted AIEgens triggered by DNAzyme cleavage for detection of PMPs. An azide-modified AIEgens (TPEN) was synthesized and conjugated to the 3' terminus of an oligonucleotide strand through an alkyl chain of 11 carbon atoms along with a planar structure (O1-TPEN) (Scheme 1A). Meanwhile, the designed THP-G4 was cleaved by DNAzyme with the cofactor Mn^{II}, resulting in the activation of tetrapod-quadruplex scaffold (TP-G4). Upon addition of O1-TPEN, the AIEgens were assembled onto the activated TP-G4 scaffold, leading to the fluorescence enhancement (Scheme 1B). The proposed strategy was applied to the detection of PMPs on living cells, providing a universal platform for PMPs detection and a proof-of concept for AIE biosensing.

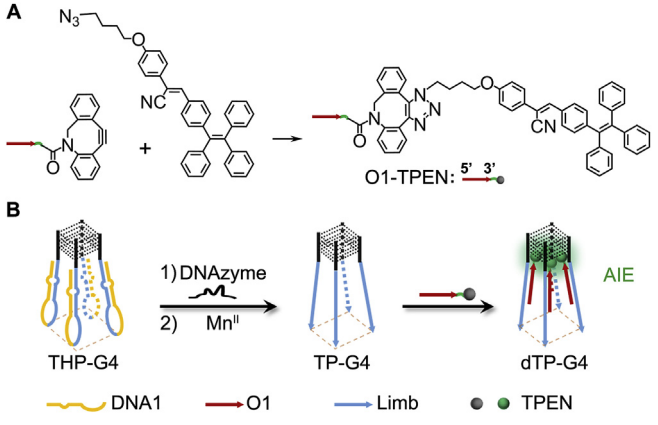

Scheme 1. Synthetic route to (A) O1-TPEN. (B) Schematic illustration of controlled assembly of AIEgens based on a super-quadruplex scaffold.

2. Materials and methods

2.1. Materials and reagents

Bromotriphenylethylene, 4-formylphenylboronic acid, tetrabutyl ammonium bromide (TBAB), tetrakis(triphenylphosphine) palladium(0) ($Pd(PPh_3)_4$), 4-hydroxybenzyl cyanide, tetrabutylammonium hydroxide, and 1,4-diiodobutane were purchased from Energy Chemical Inc. Gel electrophoresis loading buffer, streptavidin, bovine serum albumin (BSA), and polystyrene (PS) bead were from Solarbio. Co., Ltd. (Beijing, China). UltraPower dye was obtained from Bioteke, Co., Ltd. (Beijing, China). DNA ladder was from Thermo Fisher Scientific Inc. (MA, USA). Phosphate buffer saline (PBS, pH 7.4) contains 136.7 mM NaCl, 2.7 mM KCl, 8.72 mM Na_2HPO_4 and 1.41 mM KH_2PO_4. Li buffer contains 10 mM Tris-HCl, pH 7.4, 100 mM LiCl, 10 mM $MgCl_2$, and 1 mM sodium EDTA. All aqueous solutions were prepared using ultrapure water (≥18.2 MΩ cm, Milli-Q). Oligonucleotide-alkyl chain-grafted DBCO (O1-DBCO) was synthesized by Takara Bio Inc. (Dalian, China). Other DNA sequences were obtained from Sangon Biotech Co., Ltd. (Shanghai, China). These DNA sequences were listed in Table S1. To form DNA G-quadruplex structures, DNA oligonucleotides were dissolved in PBS, pH 7.4, heated to 95 °C, and cooled gradually to room temperature (0.6 °C/min), and stored at 4 °C for two days prior to use.

2.2. Apparatus

Absorption spectra were recorded on a Cary 300 UV-VIS Spectrophotometer (Agilent). The gel electrophoresis was performed on the mini-PROTEAN system (Bio-Rad) and imaged on Bio-Rad ChemDoc XRS. Fluorescence spectra were measured on an F-7000 spectrofluorophotometer (Hitachi). The dynamic light scanning (DLS) measurements were performed on 90Plus Particle Size Analyzer (Brookhaven Instruments Corporation). Circular dichroism (CD) measurements were obtained at 25 °C using 1-mm path length cuvettes (Hellma) on a Chirascan CD spectrometer (Applied Photophysics). NMR spectrum was obtain from 400 Hz spectrometer (Bruker). Matrix-assisted laser desorption/ionization time-of-fight mass spectrometry (MALDI-TOF-MS) experiments were performed on a 4800 Plus MALDI TOF Analyzer (AB Sciex).

2.3. Synthesis of TPEN

The TPEN was synthesized via four steps as shown in Scheme S1. First, according to the Suzuki coupling reaction, bromotriphenylethylene (3.0 g, 9 mmol) (**1**) and 4-formylphenylboronic acid (2.0 g, 13 mmol) were dissolved in 60 mL toluene followed by adding TBAB (0.3 g, 1.0 mmol) and 2 M potassium carbonate aqueous solution (18 mL). The mixture was stirred at room temperature for 0.5 h before adding $Pd(PPh_3)_4$ (0.010 g, 8.70×10^{-3} mmol) under Ar gas. The mixture was heated to 90 °C for 24 h, extracted with DCM and purified by column chromatography to obtain compound **2** (2.91 g, 90%) [39]. Next, according to Knoevenagel reaction, compound **2** (1 g, 2.7 mmol) and 4-hydroxybenzyl cyanide (0.45 g, 3.4 mmol) were dissolved in 30 mL ethanol before adding 5 drops of tetrabutylammonium hydroxide (0.8 M). The mixture was heated and refluxed overnight followed by washing multiple times

with ethanol to obtain compound **3** (1.10 g, 83%). The compound **3** (500 mg, 1 mmol), 1,4-diiodobutane (651 mg, 2 mmol) and potassium carbonate (290 mg, 4 mmol) were dissolved in 30 mL acetonitrile for nucleophilic substitution reaction. The mixture was heated to 80 °C and refluxed overnight and extracted with DCM and purified by column chromatography to obtain compound **4** (545 mg, 85%). Finally, compound **4** (500 mg, 0.8 mmol) and NaN_3 (160 mg, 2.5 mmol) were dissolved in 10 mL DMSO and stirred at room temperature for 24 h. The mixture was extracted with DCM and purified by column chromatography to obtain compound **5** (417 mg, 89%). ^{1}H NMR (400 MHz, CDCl3): δ 7.62 (d, J = 8.4 Hz, 2H), 7.56 (m, 2H), 7.30 (s, 1H), 7.12 (m, 11H), 7.04 (m, 6H), 6.92 (m, 2H), 4.03 (t, J = 6.0 Hz, 2H), 3.38 (t, J = 6.6 Hz, 2H), 1.89 (dt, J = 10.3, 5.7 Hz, 2H), 1.81 (m, 2H). Mass spectrum (ESI), m/z calcd for 572.258; found, 595.251 $[M+23]^+$.

2.4. Synthesis of O1-TPEN

The O1-TPEN was synthesized by mixing 0.2 mL of 100 μM O1-DBCO with 0.2 mL of 1 mg mL^{-1} TPEN in DMSO under gentle stirring at room temperature overnight. The resulting mixture was purified by Polyacrylamide Gel Electrophoresis (PAGE) with a coupling yield of 20.5% by ultraviolet absorbance analysis [40].

2.5. Fluorescence measurement

The excitation wavelength was set to 375 nm, the emission spectra were scanned from 420 to 700 nm at 25 °C. For the typical fluorescence measurements, Oligo-AIEgen (1.0 μM) was mixed with equal molar DNA strand in PBS buffer at room temperature. Unless noted, all fluorescent data were recorded at 25 °C. For the calibration curve, stock MUC1 solution was diluted to different concentration followed by incubation with capture DNA in PBS for 30 min. Then the mixture was ultrafiltration and the pellet was redispersed in PBS followed by addition of THP-G4 and Mn^{II} for 1.5 h. Then O1-TPEN was added to the ultrafiltration liquid before subjecting to fluorescence measurement.

2.6. Polyacrylamide gel electrophoresis analysis

Native polyacrylamide gel was prepared using 1 × TBE buffer. The loading sample was prepared by mixing 7 μL DNA sample, 1.5 μL 6 × loading buffer (Thermo), and 1.5 μL UltraPower dye (Bioteke). After 3 min, the samples were injected into the polyacrylamide hydrogel. The gel was operated at 100 V for 75 min in 1 × TBE buffer, and scanned with a Molecular Imager Gel Doc XR.

2.7. Cell culture and MUC1 detection

MCF-7 cells were cultured in a flask in Dulbecco's modified Eagle's medium (DMEM, Gibco), MDA-MB-231 were grown in L-15 medium. Both media were supplemented with 10% fetal calf serum (FCS, Gibco), penicillin (100 μg mL^{-1}), and streptomycin (100 μg mL^{-1}) at 37 °C in a humidified atmosphere containing 5% CO_2. Capture DNA was heated to 95 °C and slowly cooled down to room temperature. Cells and 100 nM capture DNA was added to the PBS buffer and incubated at 37 °C for 30 min followed by centrifugation and washing with PBS. Then cells were suspended in 50 μL PBS containing 0.5 mM Mn^{II} and 1 μM THP-G4. The mixture was incubated at room temperature for 1.5 h and the supernatant was obtained by centrifugation at 1000 rpm. Then, 1 μL of 50 μM O1-TPEN was added to the supernatant and incubated for 10 min before the fluorescence of resulting mixture was measured.

3. Results and discussion

3.1. Synthesis of TPEN and O1-TPEN

The designed TPEN molecule consists of two domains (Scheme S1), a green-emissive TPE derivative as the fluorescence source, and azide groups for covalent conjugation with oligonucleotides. The chemical structure of TPEN was characterized by 1H NMR and ESI-MS with high purity (Fig. S1). On the other hand, a 15 nt oligonucleotide was labelled with dibenzocyclooctyne (O1-DBCO) group on the 3' terminus (Table S1). The O1-TPEN was prepared by copper-free click reaction between O1-DBCO and TPEN (Scheme 1A and Fig. S2). The resulting O1-TPEN was purified by polyacrylamide gel electrophoresis (PAGE) and characterized by mass spectrometry with a molecular weight of 5742.7 (Fig. S3).

The TPEN in DMSO/H_2O (v/v, 1/399) exhibited two UV absorption peaks at 233 and 384 nm. After TPEN grafted with O1, the complex showed a strong absorption at 260 nm, which was in agreement with oligonucleotide absorption of O1-DBCO, suggesting the successful preparation of O1-TPEN (Fig. 1A). TPEN aggregates showed a strong fluorescence (FL) peak with maximum emission intensity at 504 nm, and maximum excitation (EX) intensity at 375 nm. After click reaction, the fluorescence intensity (F) of O1-TPEN at 504 nm was extraordinarily weakened to 3.2% of that of O1-TPEN (Fig. 1B). The hydrophobic TPEN was well dissolved in DMSO showing weak emission. As the fraction of H_2O in the mixture of DMSO/H_2O was higher than 30%, TPEN became strongly emissive, demonstrating the classic AIE property. Whereas O1-TPEN exhibited weak emission in all DMSO/H_2O mixture (Fig. 1C), indicating its good solubility in both DMSO and H_2O. TPEN formed the aggregated particles in DMSO/H_2O (v/v, 1/399) ranging from 92 to 220 nm (Fig. 1D), but O1-TPEN did not scatter light. These results suggesting that oligonucleotide grafted TPEN could well dissolve in H_2O with weak emission to provide FL-off state of O1-TPEN.

3.2. Assembly of O1-TPEN by DNA G-quaduplexes

The tetramolecular DNA G-quadruplex (TP′-G4) could assemble oligonucleotide-AIEgen in the confined space to generate fluorescence (Fig. 2A). When O1-TPEN was mixed with G-quadruplex

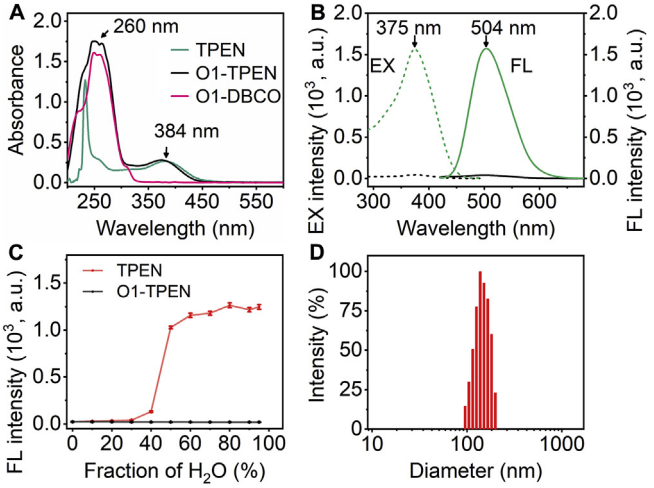

Fig. 1. (A) UV–vis spectra of 1 μM TPEN (green line), O1-TPEN (black line) and O1-DBCO (red line) in DMSO/H_2O (1/399). (B) Fluorescence spectra of 1 μM TPEN (green line), O1-TPEN (black line) in DMSO/H_2O (1/399). (C) FL intensity of TPEN and O1-TPEN versus fraction of H_2O in the mixture of DMSO/H_2O. (D) DLS measurement of TPEN in DMSO/H_2O (1/399). (For interpretation of the references to color in this figure legend, the reader is referred to the Web version of this article.)

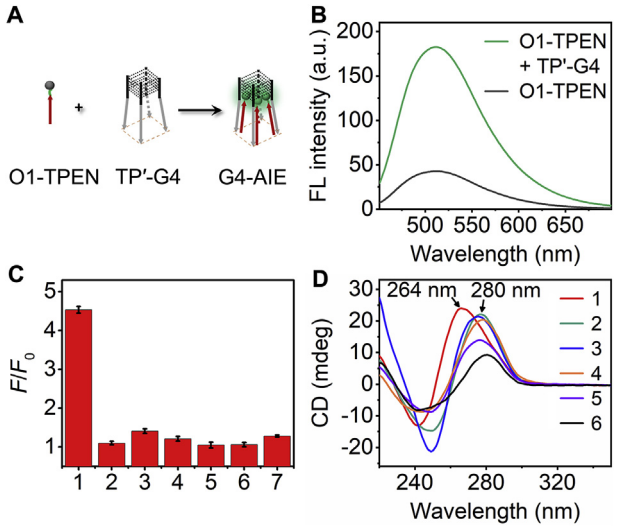

Fig. 2. (A) Schematic illustration and (B) fluorescence spectra of controlled assembly of AIEgens by G-quadruplex scaffold. (C) F/F_0 of 1 μM O1-TPEN and (D) CD spectra of 20 μM O1-TPEN with different treatments: O1-TPEN mixed with equimolar of (1) O1′-6G, (2) O1′-6T, (3) O1′-6A, (4) O1′-6C, (5) O1′, (7) 15T-6G in PBS, and (6) O1′-6G in Li Buffer. F_0 and F are the FL intensities before and after treatment, respectively.

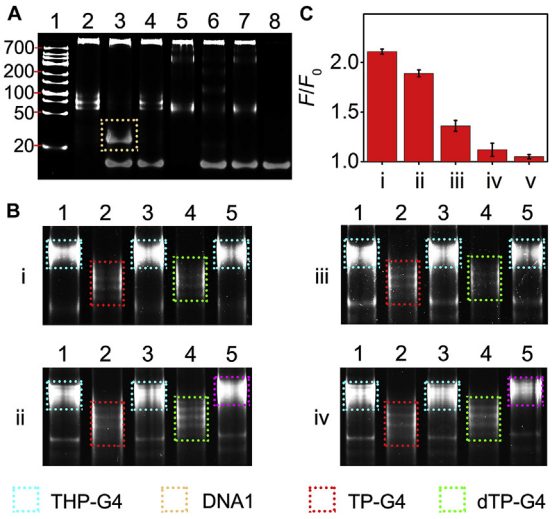

Fig. 3. (A) PAGE results (15%) of (1) DNA ladder, (2) THP-G4, (3) THP-G4 + DNAzyme + Mn^{II}, (4) THP-G4 + DNAzyme, (5) cHP, (6) cHP + DNAzyme + Mn^{II}, (7) cHP + DNAzyme, (8) DNAzyme. DNA ladder from top to bottom: 700, 500, 400, 300, 200, 150, 100, 75, 50, 25 bp. (B) PAGE results (8%) for different hairpin G-quadruplex scaffolds: (i) THP-G4, (ii) THP-G4′, (iii) THP-G4″, (iv) THP-G4‴, (v) cHP treated with (1) THP-G4, (2) THP-G4 + DNAzyme + Mn^{II}, (3) THP-G4 + DNAzyme, (4) THP-G4 + DNAzyme + Mn^{II} + O1-TPEN, (5) THP-G4 + DNAzyme + O1-TPEN. (C) Ratio of FL intensity after (F) to before (F_0) incubation of Mn^{II} in the presence of above THP-G4 scaffolds + DNAzyme, followed by addition of O1-TPEN.

scaffold (O1′-6G), the fluorescence intensity at 504 nm was enhanced as 4.5-fold of that of O1-TPEN (Fig. 2B). On contrary, the fluorescence of O1-TPEN exhibited slightly enhancement when either mixing with non-G4 oligonucleotides (O1′, O1′-6T, O1′-6A, O1′-6C), or with O1′-6G in Li buffer. Besides, 15T-6G could form G-quadruplex scaffold without complementary to O1-TPEN. The mixture of O1-TPEN and 15T-6G resulted in little fluorescence increase (Fig. 2C and Table S1). PAGE results confirmed that O1′-6G formed G-quadruplex scaffold instead of O1′, O1′-6T, O1′-6A and O1′-6C, and O1-TPEN could hybridize with G-quadruplex scaffold (Fig. S4). The circular dichroism (CD) spectra of the mixture of O1-TPEN and O1′-6G showed a positive peak at 264 nm and negative peak at 240 nm belonging to the characteristic peaks of parallel G-quadruplex. The CD spectra of mixture of O1-TPEN and other strands showed strong positive peak at 280 nm attributing to the double-stranded structure (Fig. 2D). The above data suggested that O1-TPEN could successfully hybridize with the TP′-G4 to induce fluorescence enhancement, verifying the universality of controlled assembly of AIEgens by G-quadruplex scaffold.

3.3. Design on conformation switch of THP-G4

In order to develop the molecular probe for PMPs detection, THP-G4 was designed and consisted of three elements, a substrate sequence of DNAzyme in the loop region, partial hybridization region in the stem, and six guanine nucleotides to form G-quadruplex (Fig. S5). Upon addition of DNAzyme and cofactor Mn^{II}, the RNA nucleotide in the substrate sequence was cleaved and DNA1 fragments were dehybridized from the limbs of TP-G4 due to instability of partial hybridization region separated by a 1 nucleotide (nt) bulge region in the stem. The DNAzyme was released and cut next substrate sequence to produce TP-G4 scaffold. Further addition of O1-TPEN into TP-G4 could assemble O1-TPEN in the scaffold to induce fluorescence enhancement. PAGE results showed a new band (yellow square) after addition of Mn^{II} to the mixture of THP-G4 and DNAzyme (Fig. 3A, lane 2), which was attributed to the DNA1 fragment. As the control experiment, tetramolecular hairpin-conjugated super-quadruplex scaffold without bulge region (cHP) did not show any new band in the corresponding position under the same condition of THP-G4 (Fig. 3A, lane 5). This indicated that bugle region in the stem of THP-G4 is essential for DNAzyme cleavage to release of DNA1 and activate TP-G4 scaffold at the optimal cleavage time of 1.5 h (Fig. S6).

To investigate the effect of THP-G4 structure on the fluorescence of assembly system, three kinds of THP-G4s were designed by altering the bulge region from 2 to 4 nucleotides, which were named THP-G4′, THP-G4″, THP-G4‴, respectively (Fig. S5). PAGE results revealed that DNAzyme could efficiently cleavage THP-G4 (light blue square) and produce TP-G4 (red square) (Fig. 3B, i, lane 2 and 3). When addition of O1-TPEN in the mixture of DNAzme and THP-G4 without Mn^{II}, no new band was observed (Fig. 3B, i, lane 5). This suggesting that O1-TPEN cannot hybridize with THP-G4. After Mn^{II} facilitated cleavage and addition of O1-TPEN, the resulting band (green square) was up-shifted compared to that of TP-G4 (Fig. 3B, i, lane 4), indicating the hybridization between TP-G4 and O1-TPEN. THP-G4′ had the same results as THP-G4 (Fig. 3B, ii). Although THP-G4″ proved to be cleavage by DNAzyme (Fig. 3C, iii, lane 2 and 3), addition of O1-TPEN to the mixture of DNAzyme and THP-G4-3 without Mn^{II} led to the band up-shift (purple square) (Fig. 3B, iii, lane 5). This suggested that O1-TPEN hybridized with THP-G4″ without DNAzyme cleavage, which was similar by using THP-G4‴ (Fig. 3B, iv). The above data suggested that the size of the bugle region in the stem of THP-G4 is vital on the efficiency of AIEgens assembly by G-quadruplex scaffold. Accordingly, the fluorescence enhancement became stronger as the size of bugle decreased upon addition of O1-TPEN (Fig. 3C). Therefore, THP-G4 provided an efficient scaffold to assemble the AIEgens for fluorescence enhancement.

3.4. Detection of plasma membrane protein

Based on the optimized THP-G4 structure, a PMPs detection strategy was developed (Fig. 4A). The MUC1 protein on cancer cells was labelled with capture DNA containing MUC1 aptamer, which was verified by confocal fluorescence imaging (Fig. S7). Upon

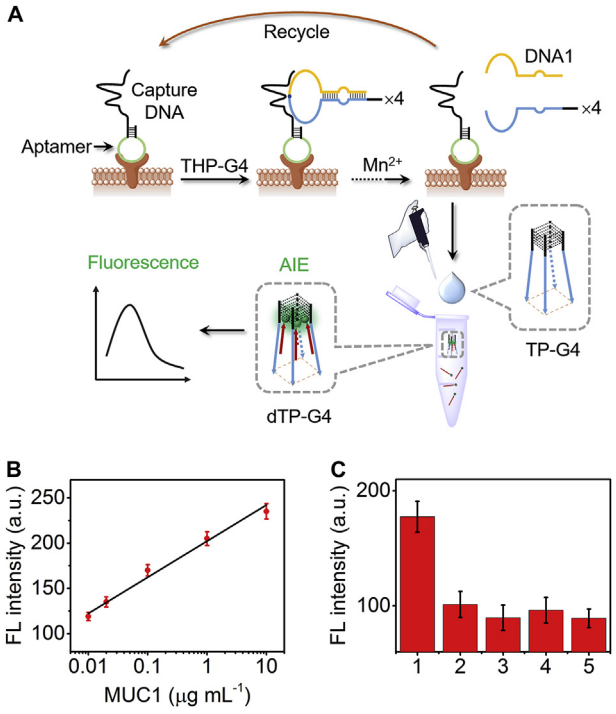

Fig. 4. (A) Schematic illustration of controlled assembly of AIEgens triggered by DNAzyme for detection of plasma membrane proteins. (B) Fluorescence calibration curve for detection of MUC1 protein. (C) Fluorescence results of the proposed strategy for detection of MUC1 on MCF-7 (1) and MDA-MB-453 (2) cells, and control experiments on MCF-7 cell labelling with aptamer (3), DNAzyme (4), aptamer-T37 (5).

addition of THP-G4 and cofactor Mn^{II} to the pretreated cells, THP-G4 was cleaved by DNAzyme, led to the activation of TP-G4 conformation. The released DNAzyme cut the next THP-G4 to generate recycling amplification. The resulting TP-G4 in the cell culture supernatant was mixed with O1-TPEN in the test tube for fluorescence assay. In order to achieve the better performance, the effect of Mn^{II} concentration and DNAzyme cleavage time was investigated. The fluorescence of the assay solution increased and plateaued when using 0.5 mM of Mn^{II} and 1.5 h of DNAzyme cleavage time, which were chosen as the optimized condition (Fig. S8). Under the optimized conditions, the fluorescence of the assay solution exhibited good linear relationship with the logarithm of MUC1 concentration from 0.01 to 10 μg mL^{-1} ($F = 39.9$ $Log(C_{MUC1}/\mu g\ mL^{-1}) + 202.2$, $R^2 = 0.988$) (Fig. 4B) with the limit of detection down to 4.3 ng mL^{-1} attributed to the DNAzyme cleavage recycle and low background of AIE signals. The detection system has good selectivity (Fig. S9), as well as lower limit of detection and wider linear range than previous fluorescence methods (Table S2). The proposed strategy was further applied to detect MUC1 on living cells. The fluorescence of assay was enhanced only by using capture DNA for cell labeling, suggesting that the strategy could selectively detect MUC1 in MCF-7 cells (Fig. 4C). Moreover, the proposed strategy can effectively detect MUC1 on MCF-7 and MDA-MB-453 cells as 105 ng mL^{-1} and 5 ng mL^{-1}, which was in agreement with previous report [18]. Thus, the proposed strategy demonstrated a universal platform for sensitive PMP detection in biological system.

4. Conclusions

This work reports a super-quadruplex scaffold for the controlled assembly of AIEgens for PMP detection. A green-emissive AIEgen was firstly synthesized and conjugated with oligonucleotide to achieve fluorescence-off state. Assembly of O1-TPEN with TP-G4 induced fluorescence enhancement to prove the universal AIE manipulation by G-quadruplex. The optimized THP-G4 could be efficiently cut by DNAzyme to activate TP-G4 conformation, resulting in hybridization with O1-TPEN to light-up fluorescence. The designed molecular switch was further applied to MUC1 detection on living cells. By replacing aptamer sequence, the proposed strategy offers a universal platform for detecting various PMPs and demonstrates a proof-of concept for AIE biosensing applications.

Declaration of competing interest

The authors declare that they have no known competing financial interests or personal relationships that could have appeared to influence the work reported in this paper.

CRediT authorship contribution statement

Longyi Zhu: Writing - original draft. **Huangxian Ju:** Writing - original draft. **Jianping Lei:** Writing - original draft.

Acknowledgments

We gratefully acknowledge National Natural Science Foundation of China (21675084, 21605082, 21890741) and Natural Science Foundation of Jiangsu Province (BK20160641).

Appendix A. Supplementary data

Supplementary data to this article can be found online at https://doi.org/10.1016/j.aca.2019.10.010.

References

[1] I.M. Ahearn, K. Haigis, D. Bar-Sagi, M.R. Philips, Regulating the regulator: post-translational modification of RAS, Nat. Rev. Mol. Cell Biol. 13 (2012) 39–51.
[2] N. Zhang, T. Bing, L.Y. Shen, R.S. Song, L.L. Wang, X.J. Liu, M.R. Liu, J. Li, W.H. Tan, D.H. Shangguan, Intercellular connections related to cell–cell crosstalk specifically recognized by an aptamer, Angew. Chem. Int. Ed. 55 (2016) 3914–3918.
[3] S. Saha, V. Prakash, S. Halder, K. Chakraborty, Y. Krishnan, A pH-independent DNA nanodevice for quantifying chloride transport in organelles of living cells, Nat. Nanotechnol. 10 (2015) 645–651.
[4] H. Li, M. Wang, T.H. Shi, S.H. Yang, J.H. Zhang, H.H. Wang, Z. Nie, A DNA-mediated chemically induced dimerization (D-CID) nanodevice for nongenetic receptor engineering to control cell behavior, Angew. Chem. Int. Ed. 57 (2018) 10226–10230.
[5] M.X. You, G.Z. Zhu, T. Chen, M.J. Donovan, W.H. Tan, Programmable and multiparameter DNA-based logic platform for cancer recognition and targeted therapy, J. Am. Chem. Soc. 137 (2015) 667–674.
[6] Z.Q.Q. Feng, H.M. Wang, S.Y. Wang, Q. Zhang, X.X. Zhang, A.A. Rodal, B. Xu, Enzymatic assemblies disrupt the membrane and target endoplasmic reticulum for selective cancer cell death, J. Am. Chem. Soc. 140 (2018) 9566–9573.
[7] M. Labib, B. Green, R.M. Mohamadi, A. Mepham, S.U. Ahmed, L. Mahmoudian, I.H. Chang, E.H. Sargent, S.O. Kelley, Aptamer and antisense-mediated two-dimensional isolation of specific cancer cell subpopulations, J. Am. Chem. Soc. 138 (2016) 2476–2479.
[8] L.C.W. Hak, S. Khan, I.D. Meglio, A.L. Law, S.L.A. Häsler, L.M. Quintaneiro, A.P.A. Ferreira, M. Krause, H.T. McMahonl, E. Boucrot, FBP17 and CIP4 recruit SHIP2 and lamellipodin to prime the plasma membrane for fast endophilin-mediated endocytosis, Nat. Cell Biol. 20 (2018) 1023–1031.
[9] J.X. Wang, M.X. Gao, G.Q. Yan, X.M. Zhang, An effective and in-situ method based tresyl-functionalized porous polymer material for enrichment and digestion of membrane proteins and its application in extraction tips, Anal. Chim. Acta 880 (2015) 77–83.
[10] Y.Z. Wu, S.G. Wu, S.Y. Ma, F. Yan, Z.Q. Weng, Cytocompatible modification of thermoresponsive polymers on living cells for membrane proteomic isolation and analysis, Anal. Chem. 91 (2019) 3187–3194.
[11] J.N. Savas, B.D. Stein, C.C. Wu, J.R. Yates III, Mass spectrometry accelerates membrane protein analysis, Trends Biochem. Sci. 36 (2011) 388–396.
[12] J. Li, Z. Skeete, S.Y. Shan, S. Yan, K. Kurzatkowska, W. Zhao, Q.M. Ngo, P. Holubovska, J. Luo, M. Hepel, C.J. Zhong, Surface enhanced Raman scattering

detection of cancer biomarkers with bifunctional nanocomposite probes, Anal. Chem. 87 (2015) 10698–10702.
[13] Y.Y. Fan, L. Li, M. Lu, H.B. Si, B. Tang, In situ fluorescent profiling of living cell membrane proteins at a single-molecule level, Chem. Commun. 55 (2019) 4043–4046.
[14] H. Liang, S. Chen, P.P. Li, L.P. Wang, J.Y. Li, J. Li, H.H. Yang, W.H. Tan, Nongenetic approach for imaging protein dimerization by aptamer recognition and proximity-induced DNA assembly, J. Am. Chem. Soc. 140 (2018) 4186–4190.
[15] S.Q. Li, Y.R. Liu, L. Lu, Y.M. Feng, L. Ding, H.X. Ju, A hierarchical coding strategy for live cell imaging of protein-specific glycoform, Angew. Chem. Int. Ed. 57 (2018) 12007–12011.
[16] X.M. Ma, Y. Lin, L.H. Guo, B. Qiu, G.N. Chen, H.H. Yang, Z.Y. Lin, A universal multicolor immunosensor for semiquantitative visual detection of biomarkers with the naked eyes, Biosens. Bioelectron. 87 (2017) 122–128.
[17] X.F. Wang, H.F. Gao, H.L. Qi, Q. Gao, C.X. Zhang, Proximity hybridization-regulated immunoassay for cell surface protein and protein-overexpressing cancer cells via electrochemiluminescence, Anal. Chem. 90 (2018) 3013–3018.
[18] T. Gao, B. Wang, L. Shi, X.L. Zhu, Y. Xiang, J.I. Anzai, G.X. Li, Ultrasensitive quantitation of plasma membrane proteins via isRTA, Anal. Chem. 89 (2017) 10776–10782.
[19] S.J. Sun, Y.N. Liu, J.L. Xia, M. Wang, R. Tang, C.Y. Lei, Y. Huang, Z. Nie, S.Z. Yao, A semisynthetic fluorescent protein assembly-based FRET probe for real-time profiling of cell membrane protease functions in situ, Chem. Commun. 55 (2019) 2218–2221.
[20] D.D. Yang, M. Liu, J. Xu, C. Yang, X.X. Wang, Y.B. Lou, N.Y. He, Z.F. Wang, Carbon nanosphere-based fluorescence aptasensor for targeted detection of breast cancer cell MCF-7, Talanta 185 (2018) 113–117.
[21] A.K.H. Cheng, H.P. Su, Y.A. Wang, H.Z. Yu, Aptamer-based detection of epithelial tumor marker mucin 1 with quantum dot-based fluorescence readout, Anal. Chem. 81 (2009) 6130–6139.
[22] J. Mei, N.C. Leung, R.T.K. Kwok, J.W.Y. Lam, B.Z. Tang, Aggregation-induced emission: together we shine, united we soar!, Chem. Rev. 115 (2015) 11718–11940.
[23] Y. Zhuang, C.L. Shang, X.D. Lou, F. Xia, Construction of AIEgens-based bioprobe with two fluorescent signals for enhanced monitor of extracellular and intracellular telomerase activity, Anal. Chem. 89 (2017) 2073–2079.
[24] J.Y. He, S.L. Gui, Y.Y. Huang, F. Hu, Y.L. Jin, G.X. Zhang, D.Q. Zhang, R. Zhao, Rapid, sensitive, and in-solution screening of peptide probes for targeted imaging of live cancer cells based on peptide recognition-induced emission, Chem. Commun. 53 (2017) 11091–11094.
[25] X.Y. Wen, Q. Wang, Z.F. Fan, An active fluorescent probe based on aggregation-induced emission for intracellular bioimaging of Zn^{2+} and tracking of interactions with single-stranded DNA, Anal. Chim. Acta 1013 (2018) 79–86.
[26] H.Y. Li, J.F. Chang, P.P. Gai, F. Li, Label-free and ultrasensitive biomolecule detection based on aggregation induced emission fluorogen via target-triggered hemin/G-quadruplex-catalyzed oxidation reaction, ACS Appl. Mater. Interfaces 10 (2018) 4561–4568.
[27] D. Mao, F. Hu, Kenry, S.L. Ji, W.B. Wu, D. Ding, D.L. Kong, B. Liu, Metal-organic-framework-assisted in vivo bacterial metabolic labeling and precise antibacterial therapy, Adv. Mater. 30 (2018) 1706831.
[28] C. Gui, E.G. Zhao, R.T.K. Kwok, A.C.S. Leung, J.W.Y. Lam, M.J. Jiang, H.Q. Deng, Y.J. Cai, W.J. Zhang, H.F. Su, B.Z. Tang, AIE-active theranostic system: selective staining and killing of cancer cells, Chem. Sci. 8 (2017) 1822–1830.
[29] Y. Cheng, J. Dai, C.L. Sun, R. Liu, T.Y. Zhai, X.D. Lou, F. Xia, An intracellular H_2O_2-responsive AIEgen for the peroxidase-mediated selective imaging and inhibition of inflammatory cells, Angew. Chem. Int. Ed. 57 (2018) 3123–3127.
[30] Q.Y. Li, X.J. Wu, X.L. Huang, Y.J. Deng, N.J. Chen, D.D. Jiang, L.L. Zhao, Z.H. Lin, Y.G. Zhao, Tailoring the fluorescence of AIE-active metal–organic frameworks for aqueous sensing of metal ions, ACS Appl. Mater. Interfaces 10 (2018) 3801–3809.
[31] D.D. Chen, H. Wang, P. Liu, L.L. Song, J.B. Shi, B. Tong, Y.P. Dong, The application of CO_2-sensitive AIEgen in studying the synergistic effect of stromal cells and tumor cells in a heterocellular system, Anal. Chim. Acta 1001 (2018) 151–157.
[32] C. Zhan, G.X. Zhang, D.Q. Zhang, Zincke's salt-substituted tetraphenylethylenes for fluorometric turn-on detection of glutathione and fluorescence imaging of cancer cells, ACS Appl. Mater. Interfaces 10 (2018) 12141–12149.
[33] Y.Y. Yuan, S.D. Xu, X.M. Cheng, X.L. Cai, B. Liu, Bioorthogonal turn-on probe based on aggregation-induced emission characteristics for cancer cell imaging and ablation, Angew. Chem. Int. Ed. 55 (2016) 6457–6461.
[34] H.B. Shi, J.Z. Liu, J.L. Geng, B.Z. Tang, B. Liu, Specific detection of integrin $\alpha_v\beta_3$ by light-up bioprobe with aggregation-induced emission characteristics, J. Am. Chem. Soc. 134 (2012) 9569–9572.
[35] M.Z. Sun, L.G. Xu, A.H. Qu, P. Zhao, T.T. Hao, W. Ma, C.L. Hao, X.D. Wen, F.M. Colombari, A.F. Moura, N.A. Kotov, C.L. Xu, H. Kuang, Site-selective photoinduced cleavage and profiling of DNA by chiral semiconductor nanoparticles, Nat. Chem. 10 (2018) 821–830.
[36] J. Chao, J.B. Wang, F. Wang, X.Y. Ouyang, E. Kopperger, H.J. Liu, Q. Li, Y.J. Shi, L.H. Wang, J. Hu, L.H. Wang, W. Huang, F.C. Simmel, C.H. Fan, Solving mazes with single-molecule DNA navigators, Nat. Mater. 18 (2019) 273–279.
[37] X.Y. Xie, Y.Q. Chai, Y.L. Yuan, R. Yuan, Dual triggers induced disassembly of DNA polymer decorated silver nanoparticle for ultrasensitive electrochemical Pb^{2+} detection, Anal. Chim. Acta 1034 (2018) 56–62.
[38] E. Largy, A. Marchand, S. Amrane, V. Gabelica, J.L. Mergny, Quadruplex turn-coats: cation-dependent folding and stability of quadruplex-DNA double switches, J. Am. Chem. Soc. 138 (2016) 2780–2792.
[39] X.Q. Zhang, Z.G. Chi, H.Y. Li, B.J. Xu, X.F. Li, W. Zhou, S.W. Liu, Y. Zhang, J.R. Xu, Piezofluorochromism of an aggregation-induced emission compound derived from tetraphenylethylene, Chem. Asian J. 6 (2011) 808–811.
[40] L.Y. Zhu, J. Zhou, G.H. Xu, C.G. Li, P.H. Ling, B. Liu, H.X. Ju, J.P. Lei, DNA quadruplexes as molecular scaffolds for controlled assembly of fluorogens with aggregation-induced emission, Chem. Sci. 9 (2018) 2559–2566.